Radiation science using Z-pinch x rays[a)]

J. E. Bailey,[1,b)] G. A. Chandler,[1] D. Cohen,[2] M. E. Cuneo,[1] M. E. Foord,[3] R. F. Heeter,[3]
D. Jobe,[4] P. W. Lake,[4] J. J. MacFarlane,[5] T. J. Nash,[1] D. S. Nielson,[4] R. Smelser,[4]
and J. Torres[1]

[1]*Sandia National Laboratories, Albuquerque, New Mexico 87185-1196*
[2]*Swarthmore College, Swarthmore, Pennsylvania 19081*
[3]*Lawrence Livermore National Laboratory, Livermore, California 94550*
[4]*K-Tech Corporation, Albuquerque, New Mexico 87185*
[5]*Prism Computational Science, Madison, Wisconsin 53703*

Present-day Z-pinch experiments generate 200 TW peak power, 5–10 ns duration x-ray bursts that provide new possibilities to advance radiation science. The experiments support both the underlying atomic and plasma physics, as well as inertial confinement fusion and astrophysics applications. A typical configuration consists of a sample located 1–10 cm away from the pinch, where it is heated to 10–100 eV temperatures by the pinch radiation. The spectrally-resolved sample-plasma absorption is measured by aiming x-ray spectrographs through the sample at the pinch. The pinch plasma thus both heats the sample and serves as a backlighter. Opacity measurements with this source are promising because of the large sample size, the relatively long radiation duration, and the possibility to measure opacities at temperatures above 100 eV. Initial opacity experiments are under way with CH-tamped NaBr foil samples. The Na serves as a thermometer and absorption spectra are recorded to determine the opacity of Br with a partially-filled *M*-shell. The large sample size and brightness of the Z pinch as a backlighter are also exploited in a novel method measuring re-emission from radiation-heated gold plasmas. The method uses a CH-tamped layered foil with $Al+MgF_2$ facing the radiation source. A gold backing layer that covers a portion of the foil absorbs radiation from the source and provides re-emission that further heats the $Al+MgF_2$. The Al and Mg heating is measured using space-resolved $K\alpha$ absorption spectroscopy and the difference between the two regions enables a determination of the gold re-emission. Measurements are also performed at lower densities where photoionization is expected to dominate over collisions. Absorption spectra have been obtained for both Ne-like Fe and He-like Ne, confirming production of the relevant charge states needed to benchmark atomic kinetics models. Refinement of the methods described here is in progress to address multiple issues for radiation science. © *2002 American Institute of Physics.* [DOI: 10.1063/1.1459454]

I. INTRODUCTION

X-ray generation, propagation, heating, and ionization contribute to the formation and evolution of many astrophysical and laboratory plasmas. Spectroscopy measurements of these plasmas provide intrinsically-interesting atomic and plasma physics. In addition, the interpretation of inertial confinement fusion (ICF) and astrophysics observations often must rely on radiation-hydrodynamic simulations. Realistic simulations depend on an accurate treatment of radiation absorption and re-emission, properties controlled by the atoms that compose the plasma. Measurements of these properties are a central aspect of radiation science. Approximations for radiation transport must often be used and the suitability of these approximations can be tested in radiation science experiments. Furthermore, plasma spectroscopy is a key diagnostic and the information quality is only as good as the atomic and plasma physics models used to interpret the data. The importance of reliable radiation science information is highest when multiple radiation hydrodynamic phenomena are intermingled. In ICF or astrophysics measurements isolating one effect from another is often not an option and those effects must be unraveled when interpreting the data. Prior radiation science experiments on isolated phenomena bolsters confidence when interpreting integrated results.

Rapid radiation science progress occurred in the last two decades[1–4] as high intensity lasers were developed and atomic models capable of analyzing complex spectra were constructed. However, the available radiation source energy has limited the experiments that were feasible. In this paper we summarize the new capability to investigate radiation science provided by the intense x-ray bursts emitted by Z-pinch plasmas at the Sandia National Laboratories Z facility.[5–7] These plasmas are presently the most energetic x-ray source available for laboratory experiments, emitting up to 1–2 MJ of x rays in a typically 6 ns full width at half maximum (FWHM) burst. The ''ride-along'' experiments described here have exposed samples with a radiation flux equivalent to a 20–70 eV blackbody. This is comparable to laser plasma
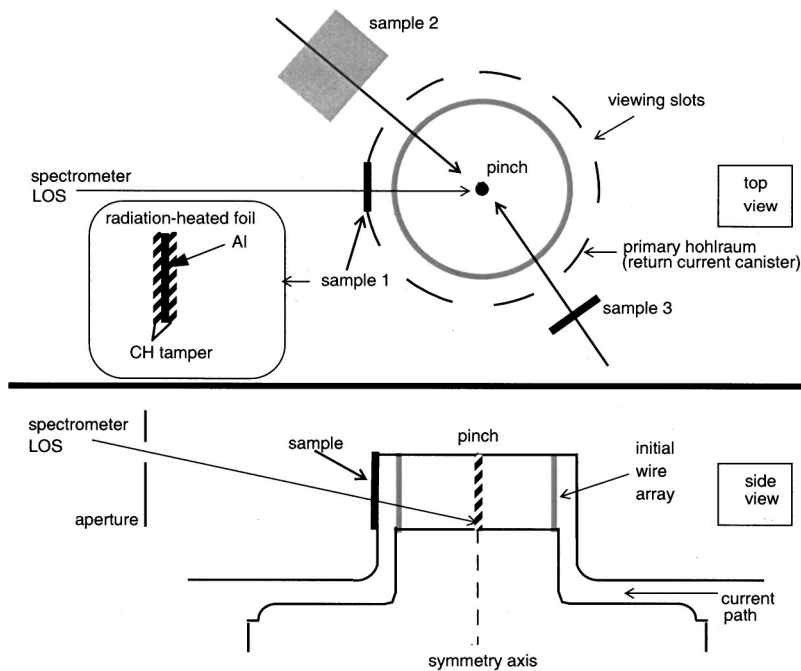
FIG. 1. Schematic diagram of radiation science experiments using the Z-pinch primary. Multiple samples located outside the primary are heated by x rays and diagnosed using the Z-pinch source as a backlighter for absorption spectroscopy.

experiments,[1–4] but the Z-pinch radiation-heated sample size and radiation duration are typically an order of magnitude larger. This promotes the ability to measure conditions in multiple samples simultaneously, to achieve more uniform conditions, and to approach closer to steady state results. As the experiment capability at Z matures, we expect that future dedicated experiments can expose samples to much higher radiation temperatures, while maintaining the characteristic large sample size and long duration.

The objective of this paper is to provide a description of the Z radiation source characteristics needed for designing radiation science experiments, illustrating the opportunities and challenges with examples of ongoing research. In Sec. II we describe the radiation intensity and spectrum obtained in the different experiment configurations, along with a very brief description of diagnostic instrumentation. Section III provides a description of $K\alpha$ satellite absorption spectroscopy measurements that are a foundation for radiation science experiments. Measurements with the simplest possible sample are used to evaluate integrated understanding of the Z radiation environment. Section IV describes a measurement of ionized bromine opacity. These bromine measurements are the focus for developing a general ability to measure opacity of open M-shell atoms. In Sec. V we describe a new method developed to measure radiation re-emission that exploits the brightness of Z as a backlighter and the benefits of large samples for simultaneously measuring transmission through multiple sample thicknesses. Section VI describes the development of Z to study atomic kinetics in photoionized plasmas. Section VII gives a brief conclusion.

II. Z RADIATION SOURCE CHARACTERISTICS

The Z radiation source is formed[5–7] by injecting an approximately 20 MA current through an annular wire array. The array is typically 20–40 mm diam, is 10–20 mm tall,

and is composed of 120–360 ~7–12 μm diam tungsten wires. The wire array is converted into a plasma and emits "run-in" radiation as it implodes. The "run-in" phase lasts for approximately 100 ns. This radiation has an equivalent blackbody brightness temperature that is initially 10–20 eV and rises to 50–60 eV just prior to stagnation. As the plasma stagnates on axis, the Z pinch emits a radiation burst. The peak power in this burst can exceed 200 TW, the duration is typically ~6 ns FWHM, the total energy is 1–2 MJ, and the spectrum is comparable to a 180–200 eV Planckian.

The return path for the injected current is a cylindrical metal canister that surrounds the pinch plasma and acts as a primary hohlraum. Diagnostic slots or holes located in the side or top of the primary enable measurements of the pinch properties. There are two classes of radiation environments available at Z: the Z-pinch primary and secondary hohlraums. In Z-pinch primary experiments (Figs. 1 and 2), samples located outside the diagnostic apertures are exposed both to direct Z-pinch radiation and to wall re-emission from the hohlraum. The spectrum therefore consists of a composite of the ~200 eV Z-pinch Planckian and the cooler emission from the primary. The radiation flux at the sample is geometrically diluted so that the incident spectrum is always harder than the spectrum of a Planckian source with a temperature equivalent to the incident flux. Geometric dilution here refers to the decrease in radiation intensity without any commensurate change in the radiation spectrum, as the sample distance from the source increases.

The Z-pinch primary geometry is conducive to performing "ride-along" experiments, where the interaction of pinch radiation with various samples can be studied using experiments with an independent main goal, such as the physics of the Z-pinch formation. Such ride-alongs have the advantage that they can examine interesting radiation physics issues without the cost associated with a dedicated experiment.
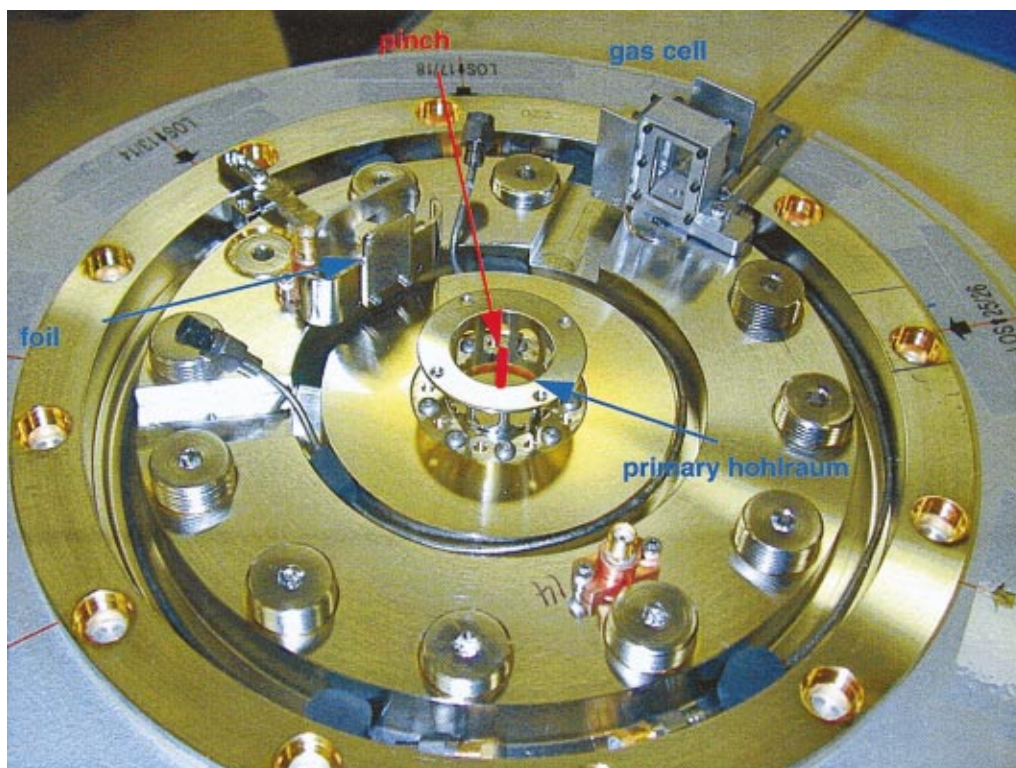
FIG. 2. (Color) Photograph of apparatus used to expose two samples to Z-pinch radiation. The approximate location of the final pinch is indicated in red.

Multiple samples can be exposed to the radiation generated in a single experiment. The disadvantages are that the radiation may not be optimized and the sample must be designed to minimize impact on the main experiment. Almost all the data reported in this paper were acquired using ride-along experiments.

The Planckian radiation spectrum required in some experiments can be achieved by using a secondary hohlraum attached to the Z-pinch primary. Secondary configurations examined at Z (Refs. 8–11) have reached radiation temperatures between 90–150 eV, for time durations of 3–30 ns. These secondaries have mainly been developed for ICF, but future radiation science experiments could exploit them.

The diagnostic suite in use at Z has been described in detail elsewhere.[12] Z diagnostics must cope with a harsh x-ray background, mechanical shock due to the dissipation of ~10 MJ of electrical energy, and debris created by the vaporization of relatively large targets. The total power and energy emerging from a diagnostic aperture is measured with filtered arrays of bolometers, x-ray diodes (XRD), calorimeters, photoconducting diodes (PCD), and Si diodes.[12–14] The power per unit area is determined by combining this measurement with time gated x-ray framing camera pictures. This enables determination of the equivalent blackbody temperature.[15] The x-ray power and spectrum are also measured with a transmission grating spectrometer.[16] The two measurements generally agree quite well.[11] Corrections to the nominal measured power are usually required. This includes accounting for the fact that 5%–20% of the total signal detected by the diagnostics is contributed by the wall re-emission rather than the pinch itself and also reduction in

the measured power due to aperture closure.[11,17,18] Uncertainties reported for the pinch emission power are approximately ±25%.[11]

The x-ray spectroscopy reported in this paper was performed using convex crystal spectrometers that provide broad spectral range and easy alignment. The brightness of the Z-pinch source allows us to overcome the low sensitivity of this geometry. A typical configuration at Z is a 25–100 mm radius crystal located ~6 m from the source. Time-integrated space-resolved spectra are recorded over a relatively large spectral range (~4–14 Å with KAP) on Kodak DEF film. The spectral resolution is typically $\lambda/\delta\lambda$ ~800–1000. Space-resolving slits provide magnification =0.5 imaged spectra with 150–1000 μm spatial resolution at the source. Time-resolved space-integrated spectra are recorded with microchannel plate (MCP)-based framing cameras. The MCP limits the spectral range and resolution to typical values of 4 Å and $\lambda/\delta\lambda$ ~500, respectively (with a KAP crystal centered at 8 Å). The time resolution of these instruments is typically ~1 ns. In recent experiments we have implemented an elliptical crystal spectrometer[19] with higher sensitivity and reduced noise due to the isolation of the detector from the line of sight. This permits simultaneous time, space, and spectral resolution.

III. RADIATION-HEATED SAMPLE DIAGNOSIS

The sample in a Z-pinch primary radiation heating experiment is exposed to a combination of direct Z-pinch emission and primary hohlraum re-emission. The relative fractions of these two components are different for the sample

Phys. Plasmas, Vol. 9, No. 5, May 2002

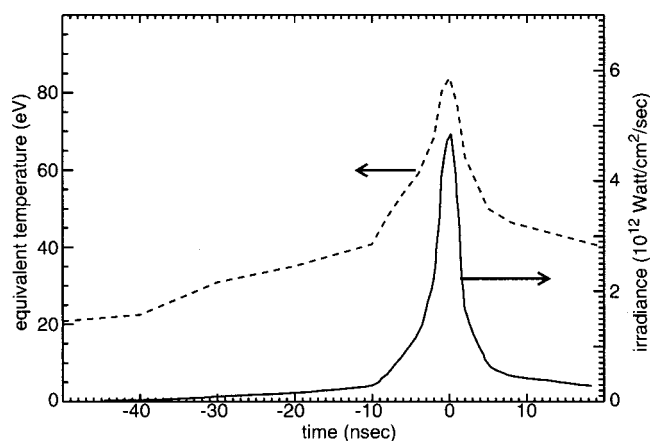Radiation science using Z-pinch x rays   2189

FIG. 3. Irradiance and equivalent blackbody temperature incident on a radiation science sample foil. The foil in this experiment was attached to the Z-pinch primary.
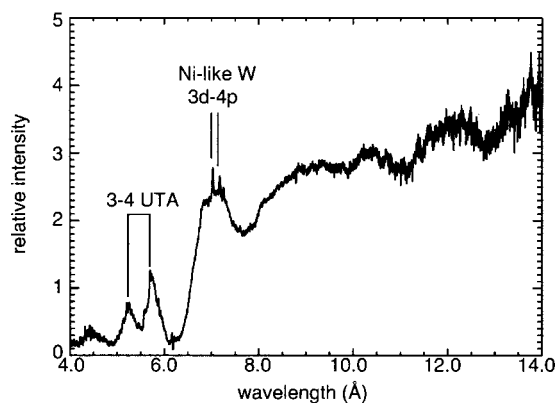

FIG. 4. Typical time-integrated x-ray spectrum emitted by a tungsten Z-pinch plasma. The quasi-continuum extending above $\lambda \sim 6.5$ Å is used as a backlighter for absorption spectroscopy.

than for the radiation source diagnostics, since the sample is typically close to the source while the diagnostics view the source on a different line of sight and from a greater distance. We therefore developed the following strategy. Starting with the measurements of the radiation source intensity, we account for the wall re-emission contribution to the radiation diagnostic signal using a view factor calculation.[20] This enables a determination of the Z-pinch emission alone. We then use a second 3D time-resolved view factor calculation to compute the radiation intensity and spectrum at the sample, from both the Z pinch itself and from the primary hohlraum re-emission. The primary hohlraum re-emission is calculated self-consistently with the pinch emission by embedding a 1D radiation-hydrodynamics calculation within each element of the view factor code. The incident irradiance and the equivalent blackbody temperature for a typical experiment are shown in Fig. 3.

The complex analysis needed to determine the incident radiation at the sample from the Z-pinch radiation measurements makes it imperative to establish the reliability of the method. This was accomplished by exposing the simplest possible sample, constructed from the best-understood element, to the Z-pinch radiation source. The sample consisted of 1000–8000 Å Al tamped on both sides by 1–4 μm CH. Al was chosen because atomic models for Al spectroscopy have been extensively developed in laser plasma[1–3,21] and ion beam[22] experiments. An x-ray spectrometer was aligned to view the pinch through the sample, so that the pinch serves to both heat the sample and as a backlighter for absorption spectroscopy (Fig. 1). The Z-pinch spectrum used for backlighting consists of a relatively-smooth quasi-continuum above 6.5 Å, along with a few Ni-like W lines and the prominent 3–4 unresolved transition arrays (UTA) in Ni-like and the adjacent charge states of W (Fig. 4). The brightness (typically ~ 200 kJ total energy above 1 keV) and the relatively-featureless spectrum above ~ 6.5 Å makes the pinch an excellent source for absorption spectroscopy. Note that the UTAs can also serve as a reasonable backlighter in the 5.1–5.8 Å region and also that care must be exercised in analysis of absorption lines in the vicinity of the $3d - 4p$ Ni-like W

transitions. Sample diagnosis was accomplished using $K\alpha$ satellite x-ray absorption spectroscopy.[23,24] $K\alpha$ satellites are $1s^2 \; 2s^l 2p^m - 1s2s^l 2p^{m+1}$ transitions that appear on the short wavelength side of the parent $K\alpha$ line associated with the neutral atom. The satellite from each charge state is shifted in wavelength because the nucleus screening changes as the number of electrons l,m in the $n = 2$ shell changes. The wavelength shift enables resolution of the transitions from different charge states and thus a measurement of the charge state distribution, which can then be related to the plasma density and temperature.

The evaluation of the sample heating understanding begins by using the incident radiation as input to a one-dimensional radiation-hydrodynamics simulation.[25] The simulation calculates the sample density and temperature as a function of time. A collisional-radiative atomic model[20,25] is then used to generate synthetic spectra that can be compared with the measured time-resolved spectra. Generally good agreement has been obtained in these comparisons. This demonstrates reasonable understanding of the integrated sample-heating problem, including the incident radiation intensity and spectrum and the response of the sample to the incident radiation. The examination of the quantitative bounds that this comparison places on our knowledge of the radiation conditions at Z will be published elsewhere. We regard this ability to be extremely important for advanced experiments using a more complicated geometry or less-well-understood elements. Therefore, we are continuing to perform similar experiments with variations in sample irradiation and fabrication that can serve to further strengthen our knowledge of the incident radiation conditions.

$K\alpha$ satellite spectroscopy is a powerful diagnostic method that is the basis for many radiation science experiments. However, the directly measured quantity is the charge state distribution. The charge state distribution is most sensitive to plasma temperature, but it also depends on the plasma density. Radiation hydrodynamic simulations can be used to provide the density, but accurate calculations are difficult and the density uncertainty can be hard to assess. The most commonly used[21] method for a density diagnostic in these types of experiments is to measure the sample expan-
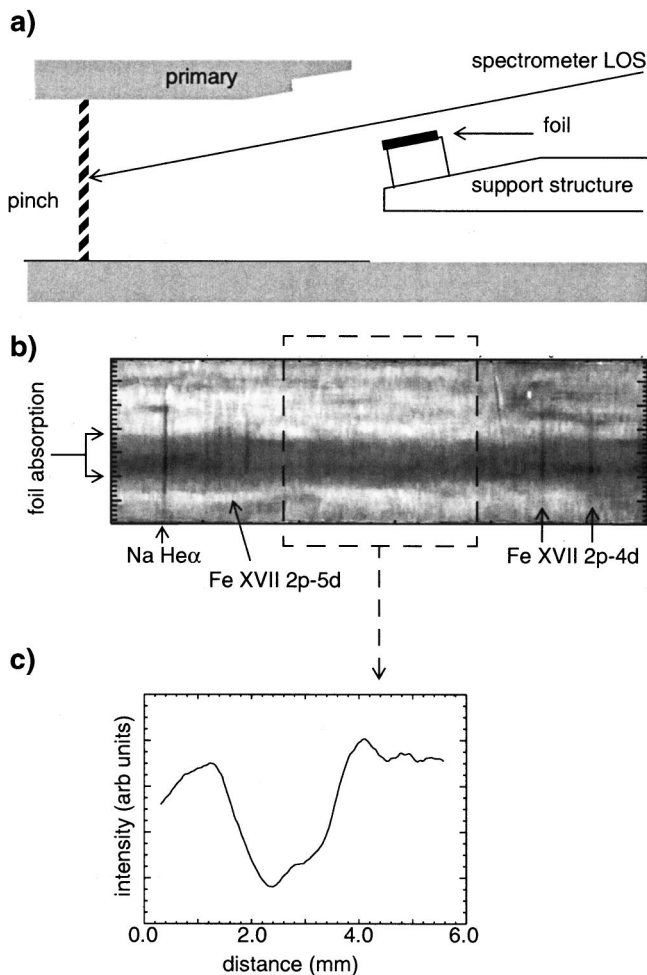
a)

b)

c)

FIG. 5. Edge-on foil experiment used to simultaneously record foil expansion and absorption spectra. The experiment geometry is shown in (a). The absorption by the expanded foil is clearly visible in a space resolved spectral image (b). A lineout across the continuum absorption (c) shows that in response to the radiation heating, the foil has expanded from its initial 500 Å thickness to approximately 2 mm.

sion. Knowing the initial sample composition and size enables determination of the density. The experiment geometry shown in Fig. 1 requires a separate backlighter/detector system operating along a line of sight parallel to the sample surface. Such measurements have not yet been performed at Z, although the recent implementation[26] of the Z beamlet laser makes future measurements feasible.

An alternative method for determining sample expansion while still permitting $K\alpha$ spectral measurements is shown in Fig. 5. We reorient the sample foil so that the surface is parallel to the diagnostic line of sight. Space-resolved spectroscopy measurements using the Z pinch as a backlighter then permit determination of the expansion and the desired absorption spectrum simultaneously. The requirement is that the foil location must be far enough from the source so that the incident radiation intensity does not vary significantly across the sample, while it must still be close enough to maintain interesting conditions. An initial proof-of-concept measurement using this technique is shown in Fig. 5. A CH-tamped sample foil was located 27 mm from the pinch. The sample was 200 Å Fe mixed with 300 Å thick NaF, with a

lateral extent along the foil surface of 2 mm. Data from this sample confirm the ability to measure the foil expansion. Detailed analysis of this experiment has not yet been performed, but the method has been applied in Fe photoionization measurements.[27]

IV. RADIATION ABSORPTION

Absorption opacities are a key to understanding radiation interaction with plasmas and provide a means of testing models for atomic physics in plasmas. Z-pinch radiation experiments offer great potential for opacity measurements. The large sample size enables simultaneous measurements through multiple sample compositions or thicknesses. The large sample size also enables measurements at low density,[28] where long path lengths are needed in order to perform an accurate transmission measurement. Planckian radiation temperatures up to $\sim$140 eV in 50 mm^3 volumes are available,[8–10] dimensions that are compatible with relatively large samples while extending the temperature range for opacity measurements by about a factor of 2–3 above prior published results (for example, see the references given in 1–4, 21). Samples with thick tamping can be probed using the Z pinch as a backlighter, possibly enabling extension of opacity measurements to higher densities than previously achieved.

The requirements of a high quality opacity experiment were described in Ref. 21. Most experiments to date, including those in this paper, have not simultaneously met all of these requirements. The experiments described here aimed at identifying the issues and problems associated with opacity experiments at Z, while providing initial measurements improving understanding of ions with a partially-filled M shell. Atoms with a partially-filled M shell were selected because calculations with such atoms are a tractable, but extremely challenging, problem for present day atomic physics models.[1–4] The experiments were performed using the ''sample 3'' configuration shown in Fig. 1. A sample consisting of 1500-Å-thick NaBr tamped by 2 microns CH on both sides was located 42 mm from the Z-pinch axis. NaBr was chosen because of the expectation that Br would be ionized into the M shell, while Na can serve as a ''thermometer'' for the plasma temperature.

The NaBr data demonstrate the utility of Z-pinch backlighter measurements with time-integrated detectors. The approximate relative time history of the blackbody temperature equivalent to the incident flux is shown in Fig. 6(a). Also shown in Fig. 6(a) is the relative time history of the Z-pinch power emitted with photon energies above 800 eV. According to these measurements, the estimated sample heating only changes by approximately ±4% during the FWHM of the keV Z-pinch backlighter emission. Therefore, measurements with time-integrated detectors should reflect conditions at the maximum temperature. This is important because the time-integrated spectrometers at Z are capable of recording both greater spectral range and superior spectral resolution data than similar time-resolved convex crystal instruments.

Phys. Plasmas, Vol. 9, No. 5, May 2002

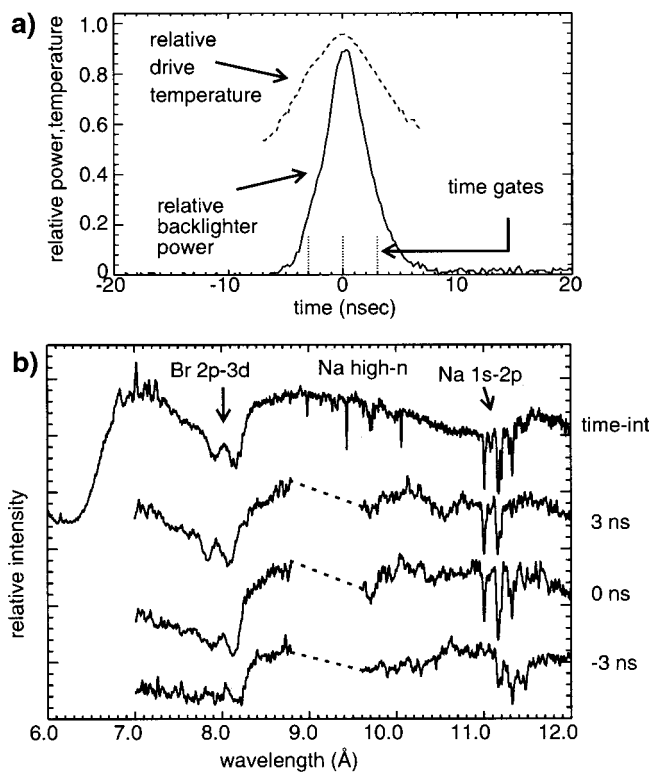Radiation science using Z-pinch x rays   2191

FIG. 6. Evolution of radiation heated foil conditions. The time history of the radiation heating drive equivalent blackbody temperature is compared with the time history of the keV Z-pinch backlighter emission in (a). A comparison of spectra recorded with time-integrated and time resolved detectors is shown in (b). The dotted lines in (a) are the gate times for the time-resolved spectra shown in (b).
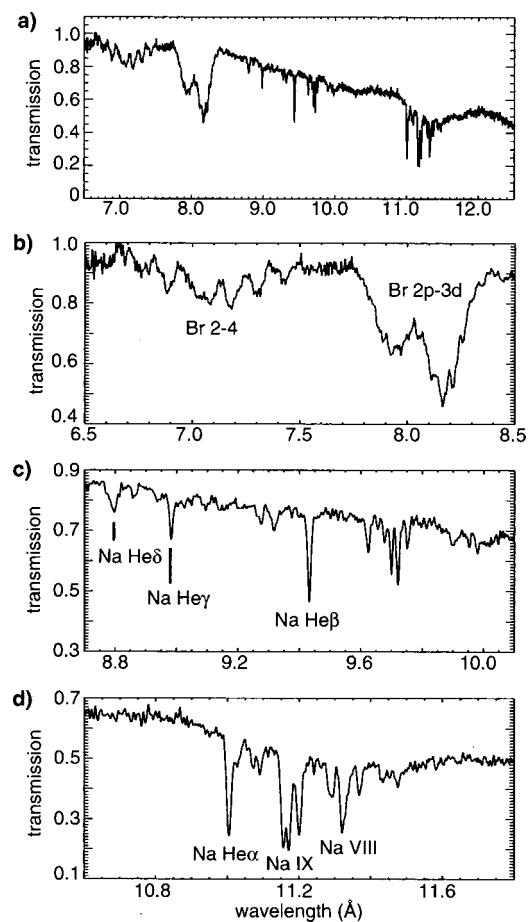

FIG. 7. Transmission measured as a function of wavelength for a radiation-heated CH-tamped NaBr sample. The entire spectrum is shown in (a) and blowups of the Br absorption lines, the Na high-n transitions, and the Na 1–2 transitions are shown in (b), (c), and (d), respectively.

A comparison of NaBr absorption spectra recorded in a single Z-pinch experiment with a time-resolved space-integrated spectrometer and a time-integrated space-resolved spectrometer is shown in Fig. 6(b). The time-resolved data used a 1.3 ns gain FWHM and a 3 ns interframe time. The frame times are indicated in Fig. 6(a). The time-resolved data between 8.8 and 9.6 Å are not displayed because a detector defect spoiled the data. We clearly observe a shift in both the Na and Br absorption features towards shorter wavelengths as the sample is heated and the ionization increases. The data recorded with the time-integrated spectrometer are very similar to the time-resolved data recorded near the peak x-ray power, as expected based on the considerations described above.

An initial measurement of the absolute spectrally-resolved transmission through the NaBr sample is shown in Fig. 7. The transmission was determined from time-integrated backlit data recorded on two essentially identical Z-pinch experiments. One experiment was performed with the NaBr sample described above and the other used no sample. The transmission was determined by dividing the two spectra, after correcting for the instrument and film response and accounting for the x-ray background. The $n=1$ to $n=2,3,4$ Na features are well-resolved and should provide an accurate sample charge state distribution measurement. An independent density measurement was not performed in this experiment. Our strategy is therefore to employ

radiation-hydrodynamic simulations using the measured radiation as input to calculate the sample density. Knowing the density, the Na absorption spectra can be used to infer the sample temperature. The density and temperature will then provide the input for an atomic physics calculation of the Br transmission. The necessity of using radiation-hydrodynamic calculations to determine the sample density is clearly not ideal, although we note that prior experiments with Al samples demonstrated good fidelity between simulated and measured Al spectra. An additional weakness is the use of separate Z-pinch experiments to determine the transmission. Nevertheless, the present results are suitable for a first order comparison of Br opacity calculations with measurements, while illuminating the improvements needed for future more stringent tests.

V. RADIATION RE-EMISSION

The efficiency of radiation absorption and re-emission governs radiative energy transport in plasmas. Re-emission is sensitive to spectrally-resolved opacity and emissivity, properties controlled by the atoms that make up the plasma. Measurements of re-emission can therefore be a useful way to test understanding of atomic properties in plasmas, while simultaneously determining one of the key quantities for ra-
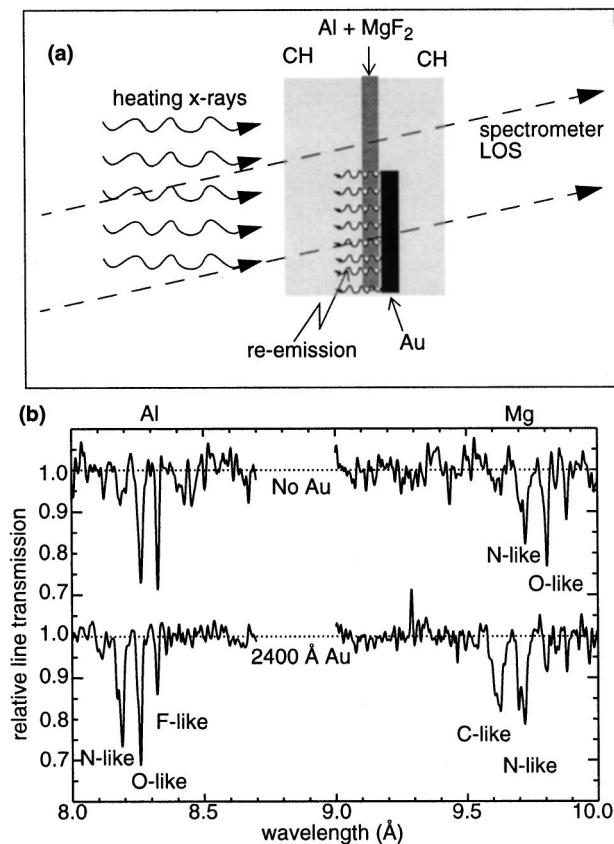
FIG. 8. Re-emission experiment. The experiment design is shown in (a). The relative line transmission is shown in (b) for the foil region without Au re-emission (top) and with Au re-emission (bottom). A clear shift in the foil ionization is caused by the Au re-emission.

diation transport.[2] Unfortunately, re-emission measurements are extremely difficult in the 10–200 Å spectral range that is the most important for typical laboratory plasmas. The re-emission measurements described here avoid this difficulty by using absorption spectroscopy at 8–10 Å in a mid-Z plasma to determine the wavelength-integrated re-emission from an adjacent high-Z plasma.

The method exploits the brightness of Z as a backlighter and the ability to measure transmission through multiple samples simultaneously. The concept is schematically illustrated in Fig. 8(a). A CH tamped sample foil is positioned outside the Z pinch (see Fig. 1). An $Al+MgF_2$ mixture fabricated by coating three alternating 250 Å thick layers, for a total thickness of 750 Å of each element, extends across the entire foil. A portion of the foil is covered with a 1600–3200 Å thick Au overcoat. The entire sample is heated by the Z-pinch primary. The blackbody temperature equivalent to the incident flux peaked at approximately 37 eV in this experiment. Part of the $Al+MgF_2$ region is also heated by re-emission from the Au backing. The temperature difference between the two regions depends on the Au opacity, the Au re-emission, and the $Al+MgF_2$ opacity in the 10–200 Å regime. The temperature difference is measured using space-resolved $K\alpha$ satellite spectroscopy of the Al and Mg lines. The challenge of successfully implementing this concept is that the Au layer must be thick enough to absorb the ~100–

1000 eV photons that provide most of the heating flux, yet we must still be able to measure an absorption spectrum at the 1200–1600 eV photon energies corresponding to the Al and Mg $K\alpha$ satellites.

Data from a proof-of-concept experiment are shown in Fig. 8(b). Spectra were recorded using a time-integrated space-resolved convex KAP crystal spectrometer with a spatial resolution of approximately 750 μm and a spectral resolution of approximately $\lambda/\delta\lambda\sim800$ in the 7–10 Å range. The FWHM of the pinch backlighter was approximately 4 ns at the relevant photon energies. Absorption spectra were recorded from the two regions and converted into relative line transmission using the procedure described in Ref. 30. A clear increase in the charge state distribution was observed in the region backed by the 2400-Å-thick Au foil. The N-like Al feature is comparable to the O-like Al feature in the Au-backed region, while the N-like Al is barely visible in the region without the Au. Similarly, the C-like Mg feature is comparable to the N-like Mg feature in the Au-backed region, while it is barely visible in the region with no Au.

The charge state increase in the Au-backed region provides qualitative proof that this concept is valuable for re-emission measurements. However, a quantitative interpretation requires detailed analysis with radiation-hydrodynamics simulations. This is essential because we must evaluate whether the density evolution in the two regions is different. The Au-backed region of the foil may tend to remain at higher density than the region without Au because of the additional tamping provided by the Au. Note that if the density is in fact higher, then the temperature difference needed to cause the observed shift in the charge state distribution is even larger. On the other hand, the higher temperature in the Au backed region may reduce the tamping effect on the density, since higher temperature will tend to cause faster expansion and lower density.

In addition to basic interest, this method may have several interesting applications. First, the use of an Au re-emission layer will reduce the temperature gradient in any absorption spectroscopy experiment with single-sided illumination by the heating x-rays. If the Au layer is thick enough, it may also help bring the test foil region (in this case, $Al+MgF_2$) electron temperature into closer equilibrium with the incident radiation temperature. Second, such foils offer a new means of reduced-leak hohlraum temperature measurements. A diagnostic aperture covered with a Au-backed $Al+MgF_2$ foil would reduce the radiation leaking out of the aperture, while still permitting temperature measurements through the analysis of the $K\alpha$ satellite spectra. Such hohlraum measurements also would not suffer from the need to apply aperture closure corrections. The principal weakness of a $K\alpha$ satellite based hohlraum temperature measurement is that the measured quantity is the charge state distribution. Therefore, we require some independent knowledge of the density. At high enough densities, it may be possible to determine the density with Stark broadening measurements.

VI. PHOTOIONIZATION

Many spectroscopy experiments have studied atomic kinetics in plasmas where the ionization distribution and ex-

cited state populations are controlled by electron collisions. In contrast, very few experiments have studied photoionized plasmas.[27,29,30] Spectroscopic measurements are needed to benchmark atomic physics models of the photoionized plasmas.[31–33] Beyond intrinsic interest in the atomic physics, these models will be applied to the interpretation of data from the new generation of satellite x-ray spectrographs that will promote the understanding of accretion-powered objects such as x-ray binaries and active galactic nuclei.[33] Moreover, this information is needed for x-ray laser research.[34–36] In this section we describe experiments aimed at determining the feasibility of benchmarking atomic kinetics models with photoionized neon and iron plasmas produced by intense Z-pinch x-ray radiation.

The lack of data from laboratory photoionized plasmas is due mainly to the need for a high intensity radiation source, as the incident radiation field must be intense enough so that photoionization dominates over collisional processes. For testing astrophysics models the ionization conditions must be comparable to astrophysical regimes, which translates into radiation fields high enough to yield dominant photoionization and into densities low enough so that 3-body recombination is small compared to dielectronic and radiative recombination. To characterize the radiation intensity we use the ionization parameter defined[31–33] as $\xi = 4\pi I/N$, where I is the irradiance at the sample expressed in erg/cm^2/s. In common usage, N is the ion density, typically approximately the same as the electron density for astrophysical plasmas due to the preponderance of hydrogen; however, here we use the electron density, since this equation is intended to reflect the balance between photoionization and recombination. The regime of interest[31–33] is $\xi \sim 1 - 1000$ erg cm/s. The ionization parameter in the experiments described here is approximately 7–50 erg cm/s.

Laboratory photoionized plasma experiments require the production of relatively low-density plasma, since the radiation intensity needed to reach a desired value of the ionization parameter is lower. Further, for astrophysics model comparisons, a density as low as possible is desirable since the density encountered in astrophysics applications is typically $10^8 - 10^{13}$ cm^{-3}. However, operating at low densities requires that the sample be large enough to provide measurable absorption or emission spectra. There are two general approaches to generating the low-density plasma. The approach used to study iron plasmas is to preheat a tamped thin foil with the low intensity x-rays from the Z run-in radiation, so that the foil expands to the desired density prior to the application of the main photoionizing radiation field. An absorption spectrum obtained with a sample configured as in Fig. 1 is shown in Fig. 9(a). The sample foil in this experiment was 200 Å Fe mixed with 300 Å NaF and tamped by 1000 Å CH on both sides. The sample was located 16 mm from the pinch axis in a dedicated experiment (the only data from a dedicated experiment shown in this paper). Absorption features from Ne-like Fe clearly appear in this spectrum, confirming that the Z radiation is sufficient to ionize the Fe into the desired charge states for testing atomic kinetics models. The required independent density measurement was not available in the initial experiments depicted in Fig. 9(a). More recent
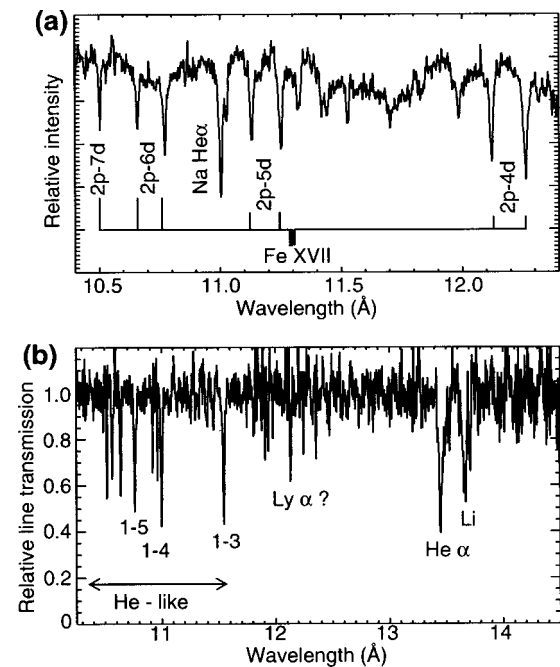

FIG. 9. Spectra from Z photoionized plasmas. An Fe plasma absorption spectrum is shown in (a) and a Ne spectrum is shown in (b).

experiments[27] have used the edge-on foil configuration shown in Fig. 5 to provide simultaneous density measurements and absorption spectroscopy data.

The second approach for photoionization experiments uses a gas cell that is filled to the desired atom density. This has the advantage that the initial atomic density is static, known, and easily adjusted to be quite low. The main disadvantage is that a thin window (typically a CH foil) must contain the gas and the hydrodynamic expansion of this window may affect the gas cell plasma. A spectrum from an initial neon-filled gas cell experiment is shown in Fig. 9(b). In this experiment we used a $1 \times 2 \times 2.34$-cm gas cell, with the 1-cm dimension oriented along the radial line of sight (LOS) to the pinch and the 2-cm dimension oriented perpendicular to the plane formed by the radial line of sight and the pinch axis. The front, rear, and one side consisted of 1.5 micron mylar windows held by a stainless steel frame with an O-ring seal The front window surface was located 57 mm from the pinch axis. The cell was filled with 30 Torr of neon, equivalent to 1.06×10^{18} atoms/cm^3. This density is at the upper limit for photoionization to dominate the ionization process. Lower densities are feasible, but the time scale for equilibrium between recombination and photoionization may then exceed the duration of the radiation pulse. The total peak irradiance at the front gas cell window was equivalent to a 48.3 eV blackbody, although the spectrum was a convolution of the pinch and wall re-emission spectra, as noted above. The irradiance at the rear gas cell boundary was calculated to be a factor of 1.5 lower, or equivalent to a 43.7 eV blackbody. The He-like and Li-like neon lines are clearly visible in the spectrum, again demonstrating that the Z radiation is intense enough to ionize neon into the desired regime.

The main result of the work presented here is that photoionized plasma experiments using the Z radiation source

are feasible. The exact relative importance of photoionization and collisions needs to be evaluated in future analysis and measurements. We believe the present absorption spectra are suitable for determining the charge state distribution and possibly the plasma temperature. However, the characterization of the plasmas needs extensive work before data will be available that can stringently constrain atomic kinetics models. The present results provide a basis for designing these future improved experiments.

VII. CONCLUSIONS

The experiment capability using Z-pinch radiation sources is rapidly evolving towards an ability to provide strong constraints on radiation science understanding. The knowledge of the incident radiation field is presently adequate and is continuing to improve. Better diagnostics for radiation science measurements are being implemented. Higher sensitivity spectrometers that allow simultaneous space, time, and spectral resolution are undergoing initial testing. The recent production of initial radiographs[37] with a plasma backlighter produced by the beamlet laser indicates that this source should be available for future radiation science experiments. The results presented here demonstrate that interesting conditions can be produced. Radiation absorption, re-emission, and photoionization are all avenues for radiation science investigations. We are also planning to broaden the scope of radiation science experiments, including radiation propagation measurements, line broadening in volumetrically heated plasmas, and using dedicated experiments to extend the range of opacity and re-emission measurements to higher temperatures and densities.

[1] R. W. Lee, Fusion Technol. **30**, 520 (1996).
[2] M. D. Rosen, Phys. Plasmas **3**, 1803 (1996).
[3] C. Chenais-Popovics, O. Rancu, P. Renaudin, and J. C. Gauthier, Phys. Scr., T **T65**, 163 (1996).
[4] E. M. Campbell, N. C. Holmes, S. B. Libby, B. A. Remington, and E. Teller, Laser Part. Beams **15**, 607 (1997).
[5] M. K. Matzen, Phys. Plasmas **4**, 1519 (1997).
[6] R. Spielmann, C. Deeney, G. A. Chandler, M. R. Douglas, D. L. Fehl, M. K. Matzen, D. H. McDaniel, T. J. Nash, J. L. Porter, T. W. L. Sanford *et al.*, Phys. Plasmas **5**, 2105 (1998).
[7] C. Deeney, M. R. Douglas, R. B. Spielman, T. J. Nash, D. L. Peterson, P. L'Eplattenier, G. A. Chandler, J. F. Seamen, and K. W. Struve, Phys. Rev. Lett. **81**, 4883 (1998).
[8] R. E. Olson *et al.*, Fusion Technol. **35**, 260 (1999).
[9] T. W. L. Sanford, R. E. Olson, R.-L. Bowers *et al.*, Phys. Rev. Lett. **83**, 5511 (1999).
[10] T. W. L. Sanford, R. E. Olson, R. C. Mock *et al.*, Phys. Plasmas **7**, 4669 (2000).
[11] M. E. Cuneo, R. A. Vesey, J. L. Porter, G. A. Chandler, D. L. Fehl, T. L. Gilliland, D. L. Hanson, J. S. McGurn, P. G. Reynolds, and L. E. Ruggles, Phys. Plasmas **8**, 2257 (2001).
[12] T. J. Nash, M. S. Derzon, G. A. Chandler *et al.*, Rev. Sci. Instrum. **72**, 1167 (2001).
[13] G. C. Idzorek and R. J. Bartlett, Proc. SPIE **3114**, 349 (1997).
[14] G. A. Chandler, C. Deeney, M. Cuneo, D. L. Fehl, J. S. McGurn, R. B. Spielman, J. A. Torres, J. L. McKenney, J. Mills, and K. W. Struve, Rev. Sci. Instrum. **70**, 561 (1999).
[15] R. B. Spielman, L. E. Ruggles, R. E. Pepping, S. P. Breeze, J. S. McGurn, and K. W. Struve, Rev. Sci. Instrum. **68**, 782 (1997).
[16] L. E. Ruggles, J. L. Porter, and R. Bartlett, Rev. Sci. Instrum. **68**, 1063 (1997).
[17] K. L. Baker, J. L. Porter, L. E. Ruggles *et al.*, Appl. Phys. Lett. **75**, 775 (1999).
[18] R. E. Chrien, W. Matsuka, G. Idzorek, F. J. Swenson, D. L. Peterson, B. H. Wilde, J. L. Porter, S. P. Breeze, L. E. Ruggles, and W. W. Simpson, Rev. Sci. Instrum. **70**, 557 (1999).
[19] B. L. Henke, H. T. Yamada, and T. J. Tanaka, Rev. Sci. Instrum. **54**, 1311 (1983).
[20] J. J. MacFarlane, J. E. Bailey, T. A. Mehlhorn, G. A. Chandler, T. J. Nash, C. Deeney, and M. R. Douglas, Rev. Sci. Instrum. **72**, 1228 (2001).
[21] T. S. Perry, P. T. Springer, D. F. Fields, D. R. Bach, F. J. D. Serduke, C. A. Iglesias, F. J. Rogers, J. K. Nash, M. H. Chen, and B. G. Wilson, Phys. Rev. E **54**, 5617 (1996).
[22] J. J. MacFarlane, P. Wang, J. E. Bailey, and T. A. Mehlhorn, J. Quant. Spectrosc. Radiat. Transf. **61**, 671 (1999).
[23] E. Nardi and Z. Zinamon, J. Appl. Phys. **52**, 7075 (1981).
[24] S. J. Davidson, J. M. Foster, C. C. Smith, K. A. Warburton, and S. J. Rose, Appl. Phys. Lett. **52**, 847 (1988).
[25] R. E. Olson and J. J. MacFarlane, Laser Part. Beams **15**, 461 (1997).
[26] G. R. Bennett, O. L. Landen, R. F. Adams, J. L. Porter, L. E. Ruggles, W. W. Simpson, and C. Wakefield, Rev. Sci. Instrum. **72**, 657 (2001).
[27] R. F. Heeter, J. E. Bailey, M. E. Cuneo, J. Emig, M. E. Foord, P. T. Springer, and R. S. Thoe, Rev. Sci. Instrum. **72**, 1224 (2001).
[28] P. T. Springer *et al.*, J. Quant. Spectrosc. Radiat. Transf. **58**, 927 (1997).
[29] J. E. Bailey *et al.*, J. Quant. Spectrosc. Radiat. Transf. **71**, 157 (2001).
[30] Y. Morita, H. Nishimura, Y. Ochi, K. Fujita, M. Fukao, M. Suzuki, T. Kawamura, H. Daido, and H. Takabe, J. Quant. Spectrosc. Radiat. Transf. **71**, 519 (2001).
[31] C. B. Tarter, W. H. Tucker, and E. E. Salpeter, Astrophys. J. **156**, 943 (1969).
[32] T. R. Kallman and R. McCray, Astrophys. J., Suppl. Ser. **50**, 263 (1982).
[33] D. A. Liedahl, Phys. Scr., T **T83**, 110 (1999).
[34] J. P. Apruzese *et al.*, in *Proceedings of the Second International Colloquium on X-Ray Lasers*, 1991, edited by G. J. Tallents (Institute of Physics, Bristol, 1991), p. 39.
[35] J. Nielsen and E. Chandler, Phys. Rev. A **44**, 4591 (1991).
[36] J. L. Porter, R. B. Spielman, M. K. Matzen, E. J. McGuire, L. E. Ruggles, M. F. Vargas, J. P. Apruzese, R. W. Clark, and J. Davis, Phys. Rev. Lett. **68**, 796 (1992).
[37] G. R. Bennett *et al.* (private communication, 2001).